Published in final edited form as:
AJR Am J Roentgenol. 2010 August ; 195(2): 341–349. doi:10.2214/AJR.09.3672.

Sodium Iodide Symporter (NIS)-Mediated Radiovirotherapy for Pancreatic Cancer

Alan R. Penheiter, Ph.D.[1], **Troy R. Wegman**[1], **Kelly L. Classic, M.S.**[2], **David Dingli, M.D., Ph.D.**[1,3], **Claire E. Bender, M.D., M.P.H.**[4], **Stephen J. Russell, M.D., Ph.D.**[1,3], and **Stephanie K. Carlson, M.D., M.S.**[1,4]

[1]Department of Molecular Medicine, 200 First Street SW, Rochester, MN 55905, Phone: 507-284-8317, Fax: 507-266-4609

[2]Section of Safety and Security, 200 First Street SW, Rochester, MN 55905, Phone: 507-284-8317, Fax: 507-266-4609

[3]Division of Hematology, 200 First Street SW, Rochester, MN 55905, Phone: 507-284-8317, Fax: 507-266-4609

[4]Department of Radiology, 200 First Street SW, Rochester, MN 55905, Phone: 507-284-8317, Fax: 507-266-4609

Abstract

OBJECTIVE—We have previously shown the therapeutic efficacy of an engineered oncolytic measles virus expressing the sodium iodide symporter reporter gene (MV-NIS) in mice with human pancreatic cancer xenografts. The goal of this study was to determine the synergy between MV-NIS-induced oncolysis and *NIS*-mediated ^{131}I radiotherapy in this tumor model.

MATERIALS AND METHODS—Subcutaneous human BxPC-3 pancreatic tumors were injected twice with MV-NIS. Viral infection, NIS expression, and intratumoral iodide uptake were quantitated with ^{123}I micro-SPECT/CT. Mice with MV-NIS infected tumors were treated with 0, 37, or 74 MBq ^{131}I and monitored for tumor progression and survival. Additional studies were performed with stable *NIS*-expressing tumors (BxPC-3-*NIS*) treated with 0, 3.7, 18.5, 37, or 74 MBq of ^{131}I.

RESULTS—Mice treated with intratumoral MV-NIS exhibited significant tumor growth delay ($p<0.01$) and prolonged survival ($p=0.02$) compared with untreated mice. Synergy between MV-NIS-induced oncolysis and *NIS*-mediated ^{131}I ablation was not seen; however, a significant correlation was observed between NIS-mediated intratumoral iodide localization (% ID/g) and peak tumor volume reduction ($p=0.04$) with combination MV-NIS and ^{131}I therapy. Stably-transduced NIS-expressing BxPC-3 tumors exhibited rapid regression with ≥18.5 MBq ^{131}I.

CONCLUSION—Delivery of ^{131}I radiotherapy to *NIS*-expressing tumors can be optimized using micro-SPECT/CT image guidance. Significant hurdles exist for *NIS* as a therapeutic gene for combined radiovirotherapy in this human pancreatic cancer model. The lack of synergy observed with MV-NIS and ^{131}I in this model was not due to a lack of radiosensitivity, but rather to a non-uniform intratumoral distribution of MV-NIS infection.

Keywords

hNIS; sodium-iodide symporter (*NIS*); ^{131}I; pancreatic cancer; measles virus

Corresponding Author: Stephanie K. Carlson, M.D., M.S., scarlson@mayo.edu.

INTRODUCTION

Pancreatic adenocarcinoma is the fourth most common cause of cancer-related death in men and women [1] and has a dismal prognosis with an overall 5-year survival rate of < 5% [2]. Conventional therapies for locally advanced, recurrent, or metastatic disease including chemotherapy, external beam radiation, or a combination of chemo-radiation therapy [3] have demonstrated minimal efficacy and are associated with considerable locoregional and systemic toxicity [4]. New targeted therapies for pancreatic cancer with increased efficacy and less toxicity are needed.

One targeted therapy that has shown great promise in numerous pre-clinical studies is the use of replicating oncolytic viruses [5–8] which also have the ability to serve as vectors for the transfer of reporter and/or therapeutic genes to infected tumor cells. A cell culture propagated molecular clone (Edm_{tag}) [9, 10] of an attenuated Edmonston vaccine lineage of measles virus has been studied extensively at our institution and has shown significant oncolytic activity in multiple tumor cell types [7, 11, 12] including pancreatic adenocarcinoma [13]. To facilitate in vivo monitoring of viral delivery and tumor response, oncolytic measles was genetically engineered to express the human thyroidal sodium-iodide symporter (MV-NIS) [14].

In addition to the role of *NIS* an imaging reporter, which has recently been validated in a human clinical trial [15], several groups have attempted to utilize *NIS* as a therapeutic transgene for tumor ablation with ^{131}I.[14, 16–21]. Early studies with doses of ^{131}I to rodents bearing *NIS*-expressing xenografts (based on mass-adjusted human maximum doses of 37–111 MBq ^{131}I/kg body mass) were unsuccessful [22–25]. However, later studies that employed much higher doses of ^{131}I (1.85–5.55 GBq/kg) have shown consistent xenograft regression (albeit at rather low calculated tumor absorbed doses of <10 Gy), in mice with stable *NIS*-expressing tumors or adenovirus transfected tumors [21, 26, 27]. These therapeutic xenograft studies provide a foundation for the concept of *NIS*-mediated isotope concentrator gene therapy, and several groups are attempting to build on this foundation by exploring strategies to trap intracellular iodide [14, 28–32].

In addition to the gene therapy approaches, a previous report from our group demonstrated a profound synergy between oncolytic MV-NIS therapy and systemically delivered ^{131}I in an multiple myeloma xenograft (MM1) model [14]. In the MM1 model, systemically delivered virus infected and replicated in the tumor, but had only a modest oncolytic effect. When 37 MBq ^{131}I was administered systemically at the peak of MV-NIS infection, the combined effects resulted in complete tumor regression in all animals. This was the first report of a synergistic relationship between an oncolytic virus (in which all *NIS*-expressing cells are destined for destruction) and systemic ^{131}I.

We previously reported the efficacy of MV-NIS virotherapy alone for the treatment of human pancreatic cancer xenografts in athymic nude mice [13]. Although therapy with MV-NIS slowed BxPC-3 human pancreatic cancer xenograft tumor growth and extended survival in mice compared with control mice, it did not completely eradicate the tumors, and there was considerable tumor-to-tumor variability in response to MV-NIS. The primary goal of the present study was to determine the synergy between MV-NIS-induced oncolysis and *NIS*-mediated ^{131}I radiotherapy in this tumor model. A secondary goal was to determine the role of micro-SPECT/CT imaging in optimizing the timing of radiovirotherapy.

MATERIALS AND METHODS

Cell Culture

BxPC-3 human pancreatic cancer cells and 293T cells were purchased from American Type Culture Collection. BxPC-3 cells were maintained in RPMI 1640 supplemented with 10% fetal bovine serum (FBS) and 1X penicillin/streptomycin cocktail. The 293T cells were maintained in Dulbecco modified Eagle medium supplemented with 10% FBS and penicillin/streptomycin cocktail. FBS was obtained from Invitrogen. All other cell culture reagents were obtained from Mediatech.

MV-NIS

A recombinant measles virus expressing the *NIS* gene was engineered at our institution and previously described [14]. The MV-NIS preparation used in all experiments in this study was produced by the Mayo Viral Vector Core [33] and contains 3.5×10^7 Vero cell tissue culture infective dose ($TCID_{50}$)/mL.

Bicistronic lentiviral vector construction and production of *NIS*-expressing BxPC-3 cell line (polymerase chain reaction [PCR]) was used to construct a self-inactivating bicistronic lentiviral vector with human *NIS* (*hNIS*) and an internal ribosome entry site (IRES)-linked emerald green fluorescence protein (Em) under the control of a spleen focus-forming virus (SFFV) promoter. Primers used were forward: 5'-AAGGATCCACCATGGAGGCCGTGGAGACCGG-3' and reverse: 5'-TTCTCGAGTCAGAGGTTTGTCTCCTG-3'. A previously constructed vector [32] was used as *hNIS* template DNA for the PCR reaction. The PCR product was cloned into pHR-SIN-B/X-IRES-Em to create plasmid pHR-SIN-*hNIS*-IRES-Em. Production of self-inactivating lentivirus was achieved using a 3 plasmid contransfection of 293T cells. Plasmids pMDG (which encodes the vesicular stomatitis virus glycoprotein under the control of a cytomegalovirus (CMV) promoter) and pCMVΔ8.91 (HIV1 gag, pol, tat, and rev) were gifts from the laboratory of D. Trono [34]. A total of 10^5 BxPC-3 cells were infected with lentivirus at a multiplicity of infection of 10, expanded to 10^7 cells, and sorted on a FACS Vantage system (Becton-Dickenson) at the Mayo Flow Cytometry/Optical Morphology Core Facility. The population of viable and fluorescent cells was sorted for emerald green fluorescence protein intensity and the sub-population that exhibited the highest 10% intensity was recovered and expanded in culture. At passage 12, BxPC-3-*hNIS*-IRES-Em cells were used for iodide uptake assays or tumor engraftment in mice, and the remaining cells were frozen in small aliquots.

Western Blot

BxPC-3-*hNIS*-IRES-Em or BxPC-3 control cells were grown to 90% confluency in a T175 flask. Cells were harvested by scraping in phosphate-buffered saline (PBS), washed twice in PBS, suspended in 1 mL radioimmunoprecipitation assay (RIPA) buffer; incubated for 15 minutes at 4°C, vortexed, and centrifuged at 15,000g. Aliquots of RIPA lysate supernatant were mixed with an equal volume of 4X reducing sodium dodecyl sulfate-loading buffer, heated to 55°C for 15 minutes, and separated on NuPage 10% Bis-Tris gels with 3-morpholino-propane sulfonic acid running buffer. Gels were then transferred to nitrocellulose membranes and probed with a mouse monoclonal antibody against the C-terminal peptide of *hNIS* (provided by Morris JC, Mayo Clinic), followed by a goat-antimouse IgG-horseradish peroxidase conjugate, and developed with an enhanced electrogenerated chemiluminescence kit. The total protein in the RIPA lysates was determined by the microbromochloroacetic acid assay.

NIS-mediated Radioiodine Uptake in Vitro

Iodide uptake assays were performed as previously described [14] using 10 kBq ^{125}I-Na.

Animal Experiments

Experiments were approved by and performed in accordance with our institutional animal care and use committee guidelines. Five- to 7-week-old female nude mice were used in all experiments (Harlan Sprague-Dawley). Mice were housed in a pathogen-free barrier facility with access to food and water ad libitum. Mice were maintained on a PicoLab 5053 mouse diet (LabDiet), which contains 0.97 ppm total iodine. One week prior to intraperitoneal administration of ^{123}I for imaging and/or ^{131}I for radiotherapy [35], 5.625 μM L-thyroxine was added to the drinking water, and mice were placed on a low-iodine diet (<0.05 ppm total iodine; Harlan Teklad). To establish xenografts, mice were inoculated subcutaneously in the right flank with 3×10^6 BxPC-3 or BxPC-3 *hNIS*-IRES-Em cells in 100-μl of PBS. Tumors were measured in two dimensions with calipers, and volume was calculated from an ellipsoid formula. Mice were observed daily and euthanized on day 90 for survival studies or immediately if they met euthanization criteria (≥15% loss of body weight, inability to access food and water, tumor ulceration, or tumor burden exceeding 2 cm^3).

Small Animal Imaging

A high-resolution micro-SPECT/CT system (X-SPECT, Gamma Medica Ideas) was used for planar and fusion micro-SPECT/CT imaging. A thorough description of the instrument can be found in the study by Carlson et al [36]. This system offers small animal functional and anatomical imaging with a micro-SPECT resolution of 3–4-mm (using a low-energy, high-resolution parallel-hole collimator with a 12.5-cm field of view) and a micro-CT resolution of approximately 155 μm. An 18.5 MBq dose of ^{123}I was administered by intraperitoneal injection to all mice 1 hour before imaging. During imaging, animals were maintained under general anesthesia with isoflurane in O_2 supplied from a veterinary vaporizer and delivered through mouse-specific nose cones. Image acquisition time was 5 minutes for planar and 13 minutes for micro-SPECT imaging (64 projections at 10 seconds per projection). Micro-CT image acquisition (155-μm slice thickness, 256 images) was performed in 1 minute at 0.25 mA and 80 kVp.

Image Analysis and Quantitation

Whole body activity (injected dose) in each mouse was determined by measuring activity in the syringe in a dose calibrator immediately prior to and after injection. Tumor activity was determined by region of interest (ROI) or volume of interest (VOI) analysis using PMOD Biomedical Image Quantification and Kinetic Modeling Software (PMOD Technologies) and previously described image analysis techniques [36]. Corresponding planar or VOI SPECT pixel counts were converted to activity using a constant derived from scanning ^{123}I standards [36]. Counts were corrected for decay, and are reported as percentage of the initial intraperitoneal injected dose. Tumor micro-SPECT activities were corrected for partial volume effect losses by application of a recovery coefficient on the basis of a previous study performed with a series of spherical phantoms containing ^{123}I [36].

Combination MV-NIS and ^{131}I Radiotherapy In Vivo

A total of 29 mice with subcutaneous BxPC-3 human pancreatic xenografts were used for the first study. When tumors reached approximately 5 mm in diameter, they were directly injected with 3.5×10^6 $TCID_{50}$/100 μL MV-NIS (n = 24 mice) or 100 μL Opti-MEM (Invitrogen) (vehicle control, n = 5 mice) using a 28-gauge needle. All tumors were injected with a second dose of virus or Opti-Mem 48 hours later. Planar mouse images were obtained with our micro-SPECT/CT scanner (1 hour after intraperitoneal injection of 18.5 MBq ^{123}I)

on day 6 after first injection of virus. Mice were injected intraperitoneal with 37 MBq or 74 MBq of ^{131}I (n = 8 mice per group) immediately after imaging and followed for tumor regression and survival for 90 days.

Serial Imaging after MV-NIS Infection

Serial imaging with ^{123}I micro-SPECT/CT on days 2, 3, 4, 6, and 9 after intratumoral MV-NIS injection (3.5×10^6 $TCID_{50}$/100 μL) was performed on eight mice with subcutaneous BxPC-3 tumors to further characterize peak intratumoral iodide localization and determine the optimal therapeutic time frame for ^{131}I administration. Mice were euthanized when their tumors showed a decrease in intratumoral iodide localization to background levels. Tumors were immediately frozen in Tissue-Tek optimum cutting temperature compound (Sakura Finetek) for immunohistochemistry analysis of intratumoral MV-NIS infection. Serial 12 μm cryosections were obtained uniformly throughout the tumor and developed with a biotinylated monoclonal antibody against measles nucleoprotein as described by Carlson et al. [13].

^{131}I Radiotherapy in Stable NIS-Expressing Tumors

To evaluate the effects of ^{131}I radiotherapy alone on BxPC-3 tumors (and thus determine their sensitivity to ^{131}I), stable *NIS*-expressing BxPC-3-*hNIS*-IRES-Em subcutaneous xenografts were established in 30 mice. This model simulates an “ideal” ^{131}I radiotherapy survival study whereby every tumor cell in the xenograft expresses *NIS*. Mice were randomly divided into groups of six on the basis of tumor size (approximately 5 mm diameter); imaged with ^{123}I micro-SPECT/CT (as described previously); and treated with 0, 3.7, 18.5, 37, or 74 MBq of ^{131}I after imaging. All mice were followed for tumor regression and survival up to 90 days. Control groups included mice with BxPC-3-*NIS* flank tumors that received no ^{131}I, and mice with BxPC-3 tumors that received 74 MBq ^{131}I.

Calculation of Absorbed Radiation Dose to Tumor Xenografts

Tumor dose in Gy was calculated for both the MV-NIS infected BxPC-3 xenografts and stable *NIS*-expressing xenografts to estimate the potential efficacy of ^{131}I radiotherapy for tumor cell killing in these tumor models. Dosimetric calculations for intratumoral ^{123}I were performed using medical internal radiation dose software and assuming a tumor density of 1 g/mL, homogeneous radionuclide distribution, a spherical shape of the tumor, and tumor effective half-life of ^{131}I of 4.5 hours [37].

Statistical Analysis

Survival curves were compared by the log-rank test using Prism version 4.03 (GraphPad Software) for Microsoft Windows to determine whether the treatment groups were significantly different from the control groups. Spearman’s correlation analyses between survival and percentage ID/g and between tumor volume and peak ^{131}I localization were performed with GraphPad Prism 4.03. Differences are considered statistically significant if $p<0.05$.

RESULTS

Combination MV-NIS and ^{131}I Radiotherapy In Vivo

Figure 1 shows representative micro-SPECT/CT images of a control mouse and an intratumoral MV-NIS infected mouse. Areas of endogenous *NIS*-mediated radioiodide uptake in the thyroid, stomach, salivary glands were observed in all mice. A strong bladder signal was observed in some mice and depended on whether the bladder was voided prior to imaging. In contrast to control tumors, significant iodide accumulation was seen in the MV-

NIS infected xenografts. MV-NIS infected tumors exhibited varying degrees of intratumoral iodide uptake with a mean (± standard error [SE]) of 8.0 ±1.3 % ID/g. The minimum and maximum uptake observed in MV-NIS infected tumors were 1.7 and 24.8 % ID/g, respectively. Control tumors not injected with MV-NIS showed normal physiologic uptake only (due to tumor vasculature and blood pooling in areas of tumor necrosis) with a mean of 1.5 ± 0.3 % ID/g and a range of 1.0 – 2.1 % ID/g.

The effects of intratumoral MV-NIS and combination intratumoral MV-NIS plus intraperitoneal ^{131}I on BxPC-3 tumor volume and mouse survival are shown in Figure 2. Two mice treated with MV-NIS only and one mouse treated with MV-NIS plus 74MBq ^{131}I survived to the end of the study (90 days). A trend of increased efficacy with combination MV-NIS plus ^{131}I therapy was observed in early tumor volume measurements (Fig. 2A); however, we did not observe a significant prolongation of survival in mice administered combination therapy versus MV-NIS alone (Fig. 2B). All treatment groups exhibited a significant ($p < 0.05$) prolongation of survival versus vehicle-injected tumors.

A trend, but not a significant correlation, was observed between tumor percentage ID/g determined by ^{123}I imaging and prolongation of survival (Fig. 3A) $n = 8$ mice injected intratumorally twice with MV-NIS and imaged 6 days after first injection). A significant negative correlation ($p = 0.04$, two-tailed) was observed between tumor volume and peak tumor uptake of ^{131}I (Fig. 3B). The calculations are based on tumor perecentage ID/g and the administered intraperitoneal dose of either 37 or 74 MBq (n=14 mice). This suggests that the reduction in tumor volume is likely due to the combined effects of MV-NIS-induced oncolysis and the antitumor effect of the administered dose of ^{131}I.

Serial Imaging after MV-NIS Infection

Serial imaging with ^{123}I micro-SPECT/CT on days 2, 3, 4, 6, and 9 after virus injection showed a considerable temporal variability in peak tumor iodide localization and tumor response following a single intratumoral MV-NIS injection (Fig. 4). Most mice exhibited peak tumor iodide localization on approximately day 6. Three of eight mice had early peak tumor iodide localization between days 2 and 4 after virus injection. By day 9, tumor signals had returned to near background levels for all mice. Interestingly, two of the three mice that displayed peak tumor iodide uptake around day 3 also exhibited complete, but markedly delayed, tumor regression. Whereas functional imaging with micro-SPECT showed an early burst of *NIS* expression and iodide uptake on day 3 after virus injection, it took more than 2 weeks for the tumors to show a significant reduction in volume as measured by micro-CT or external calipers. This likely represents a delayed clearance of viral-lysed cell debris.

In addition to variability in temporal expression of *NIS*, immunohistochemistry revealed a dramatic heterogeneity in the spatial distribution of MV-NIS infected cells within the tumor. Figure 4C shows a representative immunohistochemical section from a BxPC-3 tumor excised day 6 after virus injection. Regions of nearly uniform infection often containing several thousand cells were consistently observed. Few if any individual infected cells were observed, suggesting that MV-NIS is highly fusogenic in this tumor model. Mouse fibroblasts in the tumor capsule and within the tumor stroma appear to be resistant to viral infection, as bands of uninfected fibroblasts often were observed surrounded by infected BxPC-3 cells. These tumors were quite heterogeneous, typically with one prominent encapsulated nodule and one or more small, newly developing, adjacent nodules.

Stable BxPC-3-hNIS-IRES-Em Experiments

Stable *NIS*-expressing BxPC-3 tumors cells were produced (BxPC-3-*hNIS*-IRES-Em) (Figs. 5A&B). In vitro, these cells concentrated iodide intracellularly 101 times that of

extracellular iodide (Fig. 5 C). In vivo, BxPC-3-*hNIS*-IRES-Em tumors exhibited significant intratumoral iodide uptake (mean, 34.7 % ID/g) (Fig. 6). Compared to BxPC-3-*hNIS*-IRES-Em xenografts receiving no ^{131}I and non-transduced BxPC-3 xenografts receiving ^{131}I, a significant dose-dependent response to ^{131}I radiotherapy (tumor volume reduction and increased mouse survival) was observed in the stable *NIS*-expressing tumors (Fig. 7). Dosimetry calculations based on a tumor effective half-life of 4.5 hours yielded a mean tumor dose of 10.8 Gy per mCi (0.29 Gy/MBq) of administered ^{131}I. Tumor mass at the time of intraperitoneal ^{131}I administration was 0.35 ± 0.16 g (mean ± SD).

DISCUSSION

In a previous study, we showed that intratumoral injection of MV-NIS in human pancreatic cancer xenografts led to decreased tumor volume and prolongation of mouse survival compared with mice with control tumor xenografts, but it rarely led to complete elimination of the tumors [13]. In this report, we evaluated the addition of *NIS*-mediated ^{131}I radiotherapy to enhance the oncolytic potency of MV-NIS therapy for pancreatic cancer.

In our first in vivo experiment, we studied the effect of combination MV-NIS and ^{131}I radiotherapy (radiovirotherapy) in pancreatic cancer xenografts that had been administered intratumoral MV-NIS. Intraperitoneal ^{131}I was given on day 6 after the first injection of virus (the timing of ^{131}I therapy was based on a previous serial imaging study performed in our laboratory) [13]. Although we did see a trend towards decreased tumor volume and increased mouse survival, the tumors were not completely eradicated and there was no significant benefit of ^{131}I radiovirotherapy over MV-NIS virotherapy alone. Three possible explanations for this lack of synergy are inappropriate timing of ^{131}I administration; lack of a bystander effect from ^{131}I in certain tumor regions, particularly at the tumor periphery and in newly developing tumor nodules which were not infected; and the possibility that BxPC-3 cells are not sensitive to radiation at these dose levels. These three possible explanations were directly tested by performing a micro-SPECT/CT serial imaging study following intratumoral MV-NIS injection, documenting the intratumoral distribution of MV-NIS infection with immunohistochemistry, and by creating a stable *NIS*-expressing xenograft model whereby 100% of the BxPC-3 cells in the tumor would express *NIS*.

Effective MV-NIS oncolysis in this model results in a transient *NIS*-mediated intratumoral iodide uptake. Therefore, the timing of imaging *NIS* expression is critical. Given that we did find a significant correlation between percentage ID/g and tumor volume reduction and that tumors occasionally can be cured with MV-NIS alone, we anticipated that had we performed serial ^{123}I imaging in these mice we could have better timed the ^{131}I radiotherapy on the day of maximal *NIS* expression in each mouse. The conclusion led us to repeat our previous study and perform serial imaging in a second group of mice with pancreatic cancer xenografts after a single intratumoral MV-NIS injection. Serial imaging demonstrated maximum intratumoral iodide uptake on approximately day 3 (n = 3 mice) or day 6 (n = 5 mice) after virus injection. The mice that exhibited maximum intratumoral ^{123}I uptake on day 3 had background levels of intratumoral iodide uptake on day 6 due to cell killing by the virus. Had these mice been given ^{131}I therapy on day 6 (as we did in the radiovirotherapy study) it would have been past the peak of iodide accumulation in the tumors and the benefit of adding ^{131}I to the therapeutic protocol would be considerably reduced. This shows the considerable temporal variation in *NIS*-mediated intratumoral iodide uptake and the importance of reporter gene imaging to accurately direct the timing of additional radiotherapy, decide if additional radiotherapy would even be appropriate, and help determine an individual's specific response to therapy.

In this and other studies, we have examined more than 20 BxPC-3 tumors at various times after MV-NIS injection (day 2 – 14) by serial sectioning and immunohistochemistry with an anti-measles nucleoprotein antibody. The immunohistochemical analysis of MV-NIS infected tumors reveals patches of nearly uniform infection containing thousands of infected cells and giant syncytia (indicating that the virus is able to successfully infect human pancreatic cancer cells and that the infected cells are highly fusogenic). However, even after 6 days of infection, there appears to be little additional spread of infection to distant regions of the tumor beyond the initial zone of viral distribution from the injection. Also the propensity of mitotic activity at the periphery of these tumors appears to create a situation where the tumor grows away from the zones of central infection. While the path length of ^{131}I β particles (mean of approximately 400 μm in H_2O) may be sufficient to reach most of the non-infected cells in small tumors, geometrical dilution of radiation-induced DNA damage due to the inverse square law likely severely limits the therapeutic bystander effect in any areas of non-uniform ^{131}I uptake within the tumor.

To evaluate the effects of ^{131}I radiotherapy alone on BxPC-3 tumors (and thus determine their sensitivity to ^{131}I), stable *NIS*-expressing BxPC-3 tumors cells were produced. These cells were then used to create tumor xenografts (with 100% of the viable tumors cells expressing *NIS*) to simulate an ideal ^{131}I radiotherapy survival study. In this study, we did show a significant dose-dependent response to ^{131}I in both tumor volume reduction and mouse survival compared to BxPC-3-*hNIS*-IRES-Em xenografts receiving no ^{131}I and non-transduced BxPC-3 xenografts receiving ^{131}I. Somewhat surprisingly, all mice with the stable *NIS*-expressing tumors administered ≥ 18.5 MBq ^{131}I (estimated dose of 5.4 Gy to the tumor) exhibited rapid tumor regression. Two of the six mice administered 3.7 MBq also exhibited a delayed tumor regression. In the MV-NIS plus ^{131}I synergy study, tumors treated with 37 MBq had a mean estimated tumor dose of 3.0 Gy whereas those administered 74 MBq ^{131}I had a mean estimated tumor dose of 5.8 Gy. In contrast to the results in the stable *NIS*-expressing tumor study many of the MV-NIS + ^{131}I tumors with an absorbed dose greater than 4 Gy did not exhibit tumor regression. The direct comparison of tumor response to ^{131}I between stable NIS-expressing tumors and MV-NIS infected tumors with similar absorbed radiation doses provides further evidence for the necessity of a relatively uniform distribution of ^{131}I for a therapeutic response at these absorbed doses.

In conclusion, *NIS* appears to a valuable quantitative reporter of MV-NIS infection; however, a benefit of combination therapy with MV-NIS and ^{131}I was not observed. Further efforts aimed at optimizing both the initial distribution of virions in the tumors as well as enhancement of the propagation of virus are likely required to achieve a synergistic effect in this tumor model.

Acknowledgments

We thank our nuclear medicine technologist, Tracy Decklever, for technical expertise and imaging assistance. We thank Mark J. Federspiel for supplying MV-NIS and Yasuhiro Ikeda for supplying the lentiviral vectors. This work was supported by the National Cancer Institute (grant K08 CA103859-03A1 and grant P50 CA102701).

References

1. American Cancer Society, Inc.. Surveillance Research. 2009.
2. Kleeff J, Michalski C, Friess H, Buchler MW. Pancreatic cancer: from bench to 5-year survival. Pancreas. 2006; 33:111–118. [PubMed: 16868475]
3. Alberts SR, Gores GJ, Kim GP, et al. Treatment options for hepatobiliary and pancreatic cancer. Mayo Clin Proc. 2007; 82:628–637. [PubMed: 17493429]
4. Boz G, De Paoli A, Innocente R, et al. Radiotherapy and chemotherapy in pancreatic cancer. Topical issues and future perspectives. JOP. 2006; 7:122–130. [PubMed: 16407634]

5. Liu TC, Galanis E, Kirn D. Clinical trial results with oncolytic virotherapy: a century of promise, a decade of progress. Nat Clin Pract Oncol. 2007; 4:101–117. [PubMed: 17259931]
6. Liu TC, Kirn D. Gene therapy progress and prospects cancer: oncolytic viruses. Gene Ther. 2008; 15:877–884. [PubMed: 18418413]
7. Russell SJ, Peng KW. Measles virus for cancer therapy. Curr Top Microbiol Immunol. 2009; 330:213–241. [PubMed: 19203112]
8. Liu TC, Thorne SH, Kirn DH. Oncolytic adenoviruses for cancer gene therapy. Methods Mol Biol. 2008; 433:243–258. [PubMed: 18679628]
9. Radecke F, Spielhofer P, Schneider H, et al. Rescue of measles viruses from cloned DNA. Embo J. 1995; 14:5773–5784. [PubMed: 8846771]
10. Combredet C, Labrousse V, Mollet L, et al. A molecularly cloned Schwarz strain of measles virus vaccine induces strong immune responses in macaques and transgenic mice. J Virol. 2003; 77:11546–11554. [PubMed: 14557640]
11. Blechacz B, Russell SJ. Measles virus as an oncolytic vector platform. Curr Gene Ther. 2008; 8:162–175. [PubMed: 18537591]
12. Msaouel P, Dispenzieri A, Galanis E. Clinical testing of engineered oncolytic measles virus strains in the treatment of cancer: an overview. Curr Opin Mol Ther. 2009; 11:43–53. [PubMed: 19169959]
13. Carlson SK, Classic KL, Hadac EM, et al. Quantitative molecular imaging of viral therapy for pancreatic cancer using an engineered measles virus expressing the sodium-iodide symporter reporter gene. AJR Am J Roentgenol. 2009; 192:279–287. [PubMed: 19098211]
14. Dingli D, Peng KW, Harvey ME, et al. Image-guided radiovirotherapy for multiple myeloma using a recombinant measles virus expressing the thyroidal sodium iodide symporter. Blood. 2004; 103:1641–1646. [PubMed: 14604966]
15. Barton KN, Stricker H, Brown SL, et al. Phase I study of noninvasive imaging of adenovirus-mediated gene expression in the human prostate. Mol Ther. 2008; 16:1761–1769. [PubMed: 18714306]
16. Blechacz B, Splinter PL, Greiner S, et al. Engineered measles virus as a novel oncolytic viral therapy system for hepatocellular carcinoma. Hepatology. 2006; 44:1465–1477. [PubMed: 17133484]
17. Chen L, Altmann A, Mier W, et al. Radioiodine therapy of hepatoma using targeted transfer of the human sodium/iodide symporter gene. J Nucl Med. 2006; 47:854–862. [PubMed: 16644756]
18. Dwyer RM, Bergert ER, O'Connor MK, Gendler SJ, Morris JC. Adenovirus-mediated and targeted expression of the sodium-iodide symporter permits in vivo radioiodide imaging and therapy of pancreatic tumors. Hum Gene Ther. 2006; 17:661–668. [PubMed: 16776574]
19. Spitzweg C, Baker CH, Bergert ER, O'Connor MK, Morris JC. Image-guided radioiodide therapy of medullary thyroid cancer after carcinoembryonic antigen promoter-targeted sodium iodide symporter gene expression. Hum Gene Ther. 2007; 18:916–924. [PubMed: 17931047]
20. Spitzweg C, Dietz AB, O'Connor MK, et al. In vivo sodium iodide symporter gene therapy of prostate cancer. Gene Ther. 2001; 8:1524–1531. [PubMed: 11704812]
21. Spitzweg C, O'Connor MK, Bergert ER, Tindall DJ, Young CY, Morris JC. Treatment of prostate cancer by radioiodine therapy after tissue-specific expression of the sodium iodide symporter. Cancer Res. 2000; 60:6526–6530. [PubMed: 11103823]
22. Shimura H, Haraguchi K, Miyazaki A, Endo T, Onaya T. Iodide uptake and experimental 131I therapy in transplanted undifferentiated thyroid cancer cells expressing the Na+/I- symporter gene. Endocrinology. 1997; 138:4493–4496. [PubMed: 9322970]
23. Mandell RB, Mandell LZ, Link CJ Jr. Radioisotope concentrator gene therapy using the sodium/iodide symporter gene. Cancer Res. 1999; 59:661–668. [PubMed: 9973215]
24. Nakamoto Y, Saga T, Misaki T, et al. Establishment and characterization of a breast cancer cell line expressing Na+/I- symporters for radioiodide concentrator gene therapy. J Nucl Med. 2000; 41:1898–1904. [PubMed: 11079502]
25. Boland A, Ricard M, Opolon P, et al. Adenovirus-mediated transfer of the thyroid sodium/iodide symporter gene into tumors for a targeted radiotherapy. Cancer Res. 2000; 60:3484–3492. [PubMed: 10910060]

26. Dingli D, Diaz RM, Bergert ER, O'Connor MK, Morris JC, Russell SJ. Genetically targeted radiotherapy for multiple myeloma. Blood. 2003; 102:489–496. [PubMed: 12649158]
27. Spitzweg C, Harrington KJ, Pinke LA, Vile RG, Morris JC. Clinical review 132: The sodium iodide symporter and its potential role in cancer therapy. J Clin Endocrinol Metab. 2001; 86:3327–3335. [PubMed: 11443208]
28. Derbre S, Lecat-Guillet N, Pillon F, Ambroise Y. Synthesis and evaluation of photoreactive probes to elucidate iodide efflux in thyrocytes. Bioorg Med Chem Lett. 2009; 19:825–827. [PubMed: 19103483]
29. Lecat-Guillet N, Merer G, Lopez R, Pourcher T, Rousseau B, Ambroise Y. Small-molecule inhibitors of sodium iodide symporter function. Chembiochem. 2008; 9:889–895. [PubMed: 18307189]
30. Elisei R, Vivaldi A, Ciampi R, et al. Treatment with drugs able to reduce iodine efflux significantly increases the intracellular retention time in thyroid cancer cells stably transfected with sodium iodide symporter complementary deoxyribonucleic acid. J Clin Endocrinol Metab. 2006; 91:2389–2395. [PubMed: 16537683]
31. Huang M, Batra RK, Kogai T, et al. Ectopic expression of the thyroperoxidase gene augments radioiodide uptake and retention mediated by the sodium iodide symporter in non-small cell lung cancer. Cancer Gene Ther. 2001; 8:612–618. [PubMed: 11571539]
32. Dingli D, Russell SJ, Morris JC 3rd. In vivo imaging and tumor therapy with the sodium iodide symporter. J Cell Biochem. 2003; 90:1079–1086. [PubMed: 14635183]
33. Hasegawa K, Pham L, O'Connor MK, Federspiel MJ, Russell SJ, Peng KW. Dual therapy of ovarian cancer using measles viruses expressing carcinoembryonic antigen and sodium iodide symporter. Clin Cancer Res. 2006; 12:1868–1875. [PubMed: 16551872]
34. Zufferey R, Dull T, Mandel RJ, et al. Self-inactivating lentivirus vector for safe and efficient in vivo gene delivery. J Virol. 1998; 72:9873–9880. [PubMed: 9811723]
35. Wollman SH, Reed FE. Kinetics of accumulation of radioiodine by thyroid gland: short time intervals. Am J Physiol. 1962; 202:182–188. [PubMed: 14008092]
36. Carlson SK, Classic KL, Hadac EM, et al. In vivo quantitation of intratumoral radioisotope uptake using micro-single photon emission computed tomography/computed tomography. Mol Imaging Biol. 2006; 8:324–332. [PubMed: 17053863]
37. Petrich T, Helmeke HJ, Meyer GJ, Knapp WH, Potter E. Establishment of radioactive astatine and iodine uptake in cancer cell lines expressing the human sodium/iodide symporter. Eur J Nucl Med Mol Imaging. 2002; 29:842–854. [PubMed: 12111124]

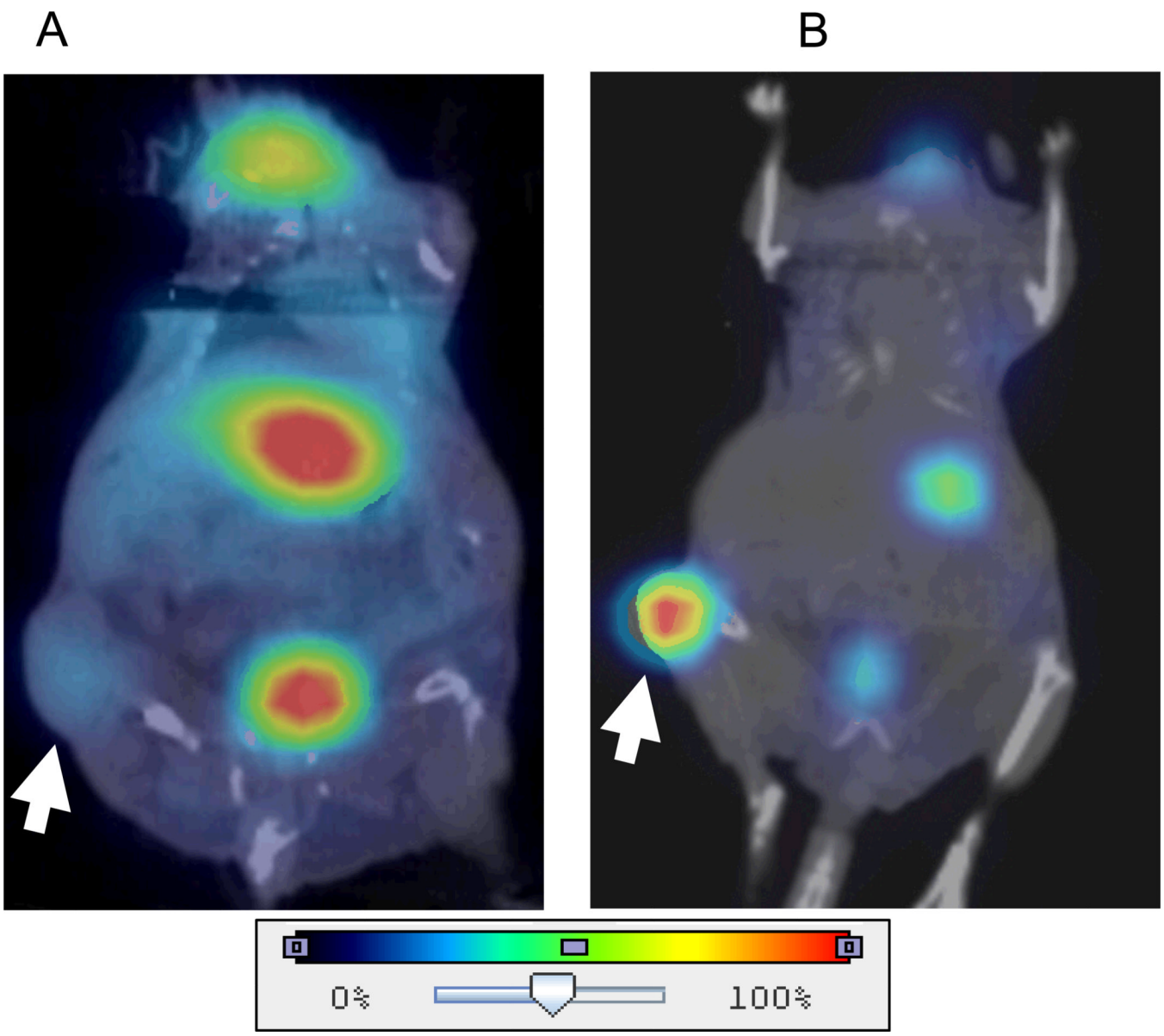

Fig. 1. Representative ^{123}I micro-SPECT/CT images of BxPC-3 flank tumor-bearing nude mice

A, Normal physiologic uptake only (arrow) (due to tumor vasculature and blood pooling in areas of tumor necrosis) was seen in the untreated control tumors. Also note areas of endogenous *NIS*-mediated radioiodide uptake in the thyroid, stomach, and accumulation in the bladder. B, In contrast, significant iodide accumulation (arrow) was seen in the MV-NIS infected xenografts.

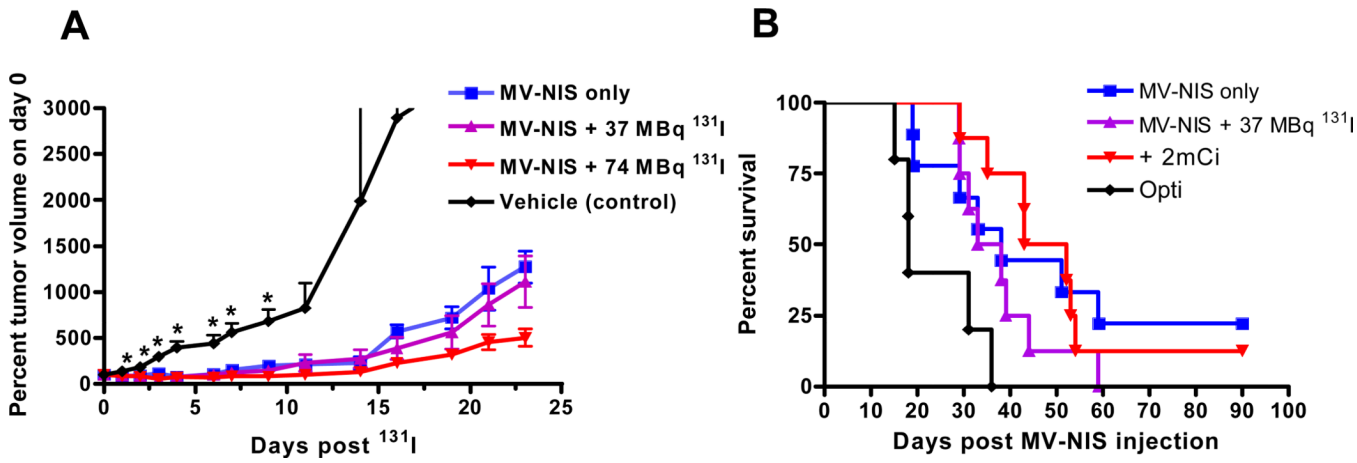

Fig. 2. Tumor volume measurements and survival analysis

A and **B,** Graphs show effect of intratumoral MV-NIS and intratumoral MV-NIS plus intraperitoneal ^{131}I on BxPC-3 tumor volume (**A**) and mouse survival (**B**). Tumors were injected with 3.5×10^6 MV-NIS or Opti-MEM (Invitrogen) (vehicle control) on day 0 and day 2. Mice were injected intraperitoneally with 37 MBq or 74 MBq of ^{131}I on day 6. Survival experiment was terminated on day 90. Tumor volume measurements are plotted to day 24 after ^{131}I (day 30 aftert MV-NIS) when only one control mouse remained in the study. Tumor volumes in all treated mouse groups were significantly different than control mice ($p < 0.01$; *asterisks*,**A**) from day 2 to day 9, when the first control mouse reached euthanization criteria. Mice were euthanized when tumor volumes reached 2 cm^3 or if the tumor exhibited severe lysis due to rapid tumor growth. Mice per group: MV-NIS only (n = 8); MV-NIS plus 37 MBq ^{131}I (n = 8); MV-NIS plus 74 MBq ^{131}I (n = 8); vehicle control (n = 5).

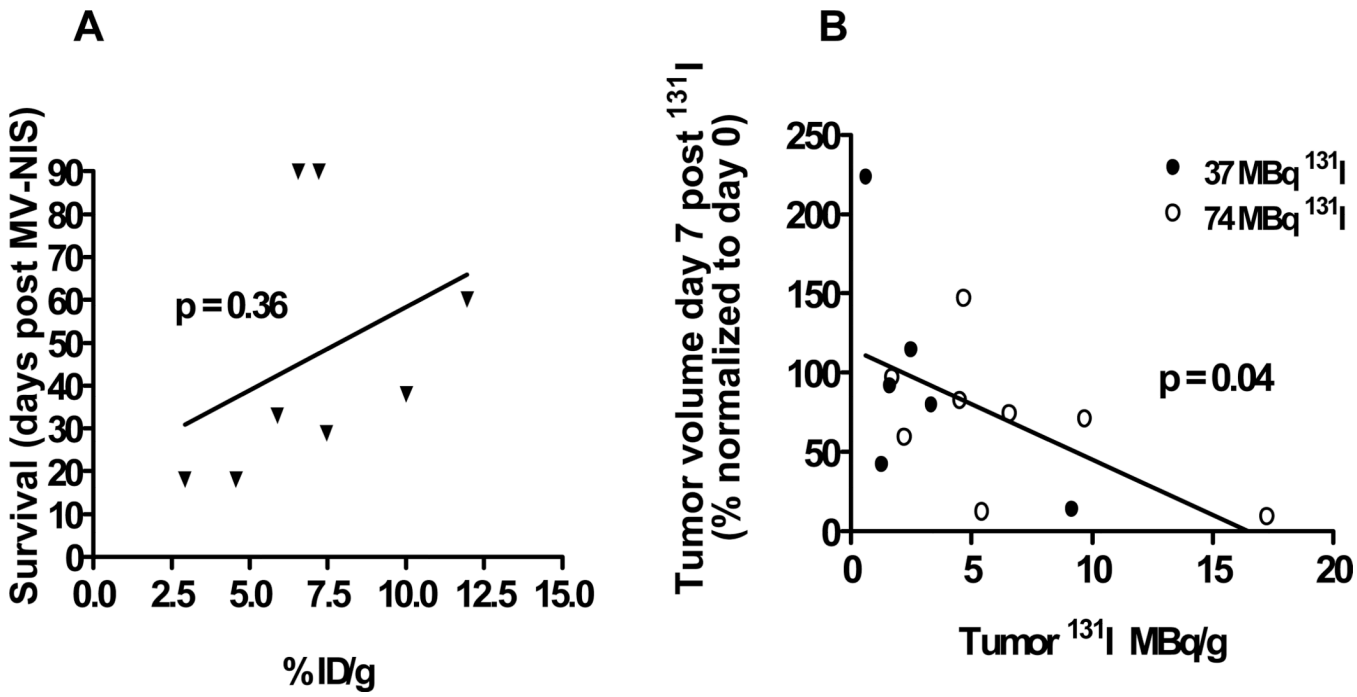

Fig. 3. Correlation for treatment with MV-NIS

A, graph shows correlation between survival and iodide localization in MV-NIS-only treated tumors (not administered ^{131}I). **B,** Correlation between day 7 tumor volume reduction and peak (1 hour after administration) ^{131}I localization in tumors treated with MV-NIS plus ^{131}I. Two mice were unable to be imaged and their uptake results are therefore not included in this analysis.

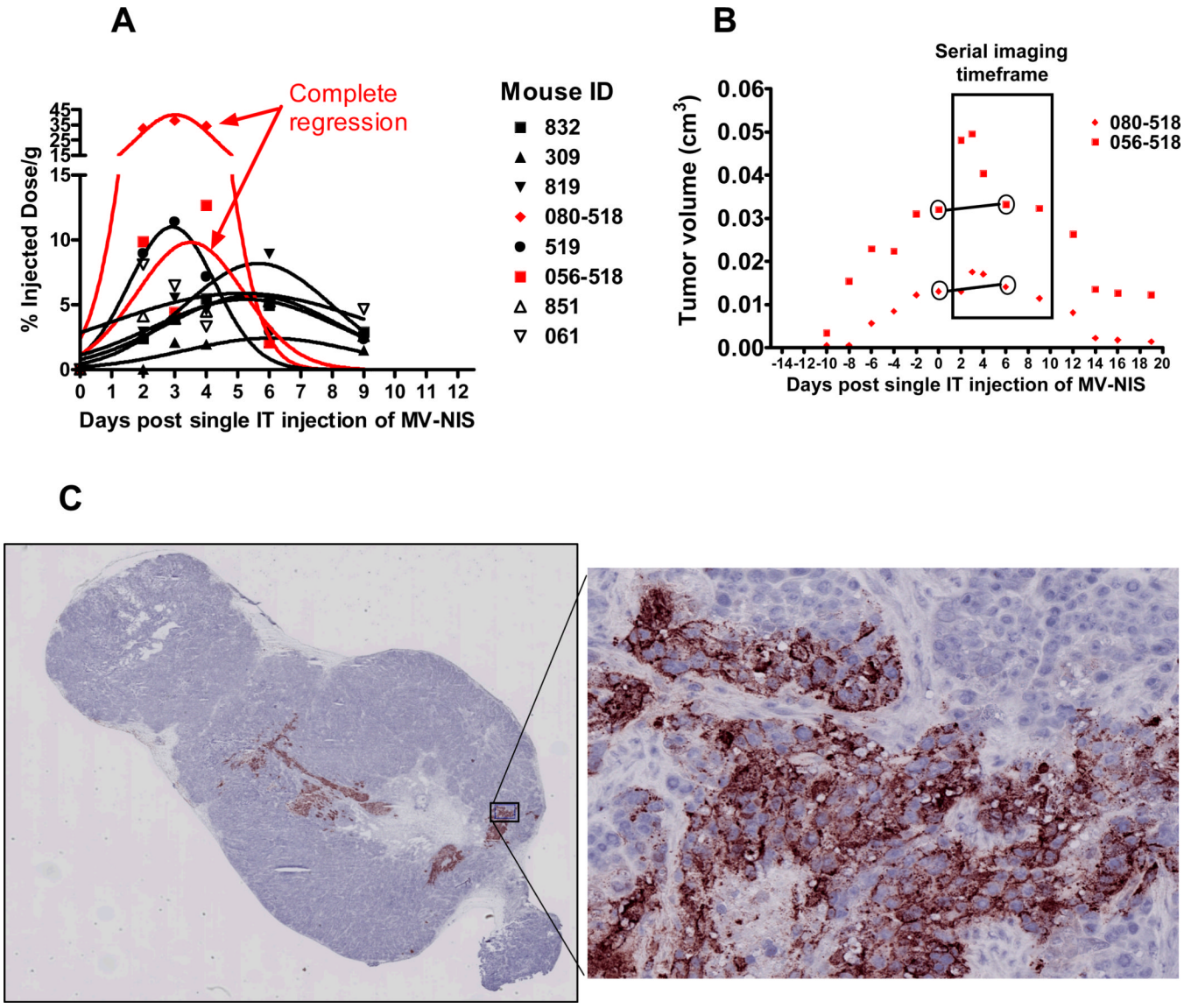

Fig. 4. Serial imaging and immunohistochemistry

^{123}I micro-SPECT/CT was performed on days 2, 3, 4, 6, and 9 after intratumoral injection of a single dose of 3.5×10^6 MV-NIS (n = 8 mice). **A**, Intratumoral iodide localization (% ID/g) was variable with 3 mice showing peak uptake on days 2–4 and five mice showing peak uptake closer to day 6. **B**, Two mice exhibited complete tumor regression after MV-NIS infection, although tumor shrinkage (measured by micro-CT and external calipers) was markedly delayed relative to the early burst of peak intratumoral iodide localization 72 hours after virus injection. **C**,. Immunohistochemistry of a representative12 μM frozen section obtained on day 6 after MV-*NIS*, incubated with a monoclonal antibody against the measles nucleoprotein, and counterstained with hematoxylin shows infected areas of tumor stain reddish-brown (*arrows*). Enlarged region shows characteristic clustering of intensely hematoxylin-stained nuclei (syncytia) in regions of the tumor infected by MV-NIS.

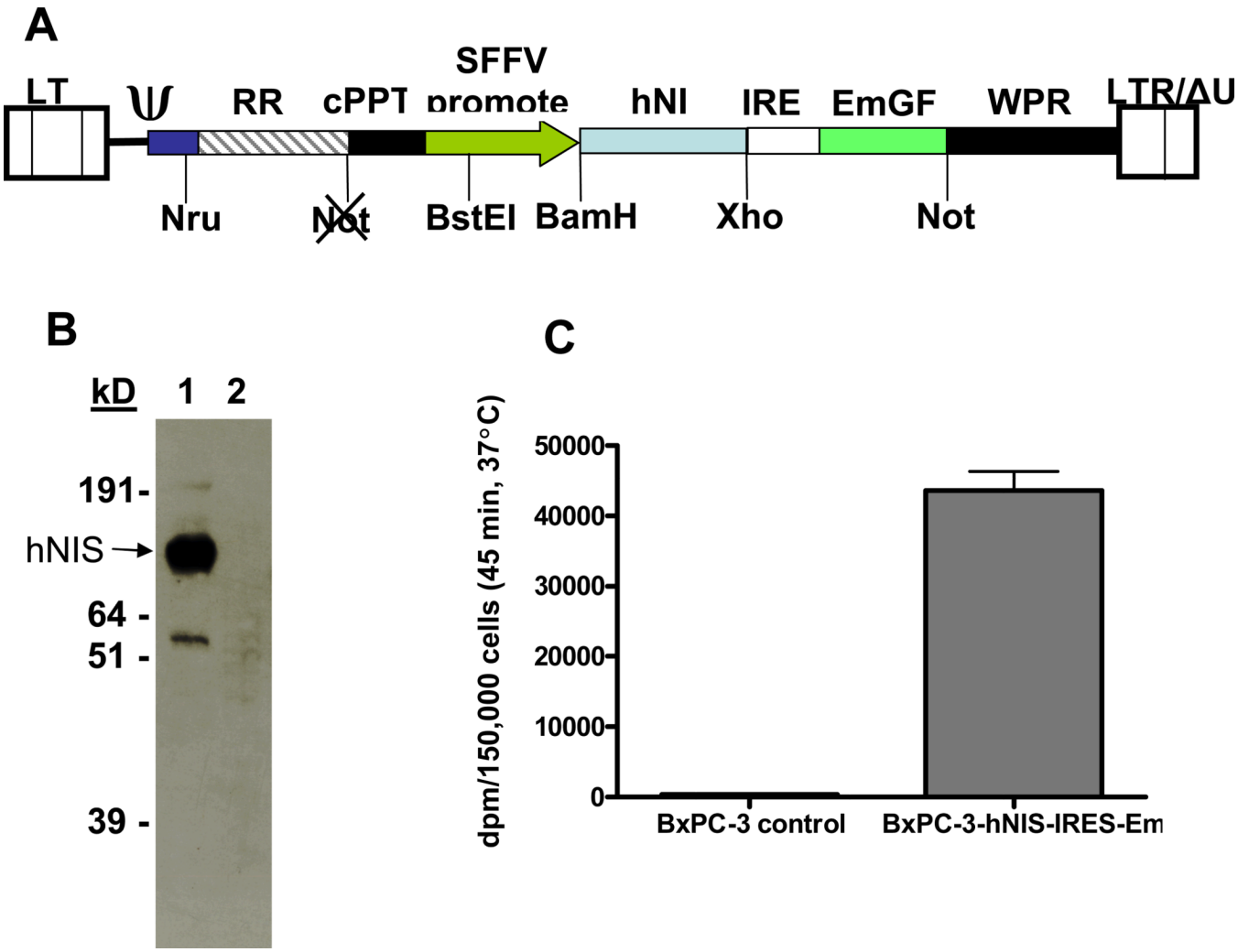

Fig. 5. Construction and in vitro characterization of BxPC-3 *hNIS*-IRES-Em cells

A,. Schematic representation of pHR-SIN-*hNIS*-IRES-Em, a self-inactivating, bi-cistronic lentiviral transfer vector used to create BxPC-3 cells which stably express the human sodium iodide symporter and a green fluorescent protein under control of spleen focus forming virus (SFFV) promoter. LTR = long terminal repeat, RRE = HIV rev response element, cPPT = central polypurine tract, *hNIS*, human sodium iodide symporter (SLC5A5), IRES = internal ribosome entry site, EmGFP = emerald enhanced green fluorescent protein, WPRE = woodchuck hepatitis virus posttranscriptional regulatory element, ΔU3 = deletion of U3 region. **B**, Graph shows Western blot of BxPC-3-*hNIS*-IRES-Em cells (26 μg total protein; lane 1) and control, nontransduced BxPC-3 cells (45 μg total protein; lane 2). **C**, Graph shows iodide uptake of BxPC-3 control cells and BxPC-3-*hNIS*-IRES-Em cells; 150,000 cells were incubated for 45 minutes at 37 °C in the presence of 17.8 kBq ^{125}I-Na. on basis of cell volume of 3.566 pL, the BxPC-3-*hNIS*-IRES-Em cells accumulated ^{125}I to a level 101 times that of external concentration.

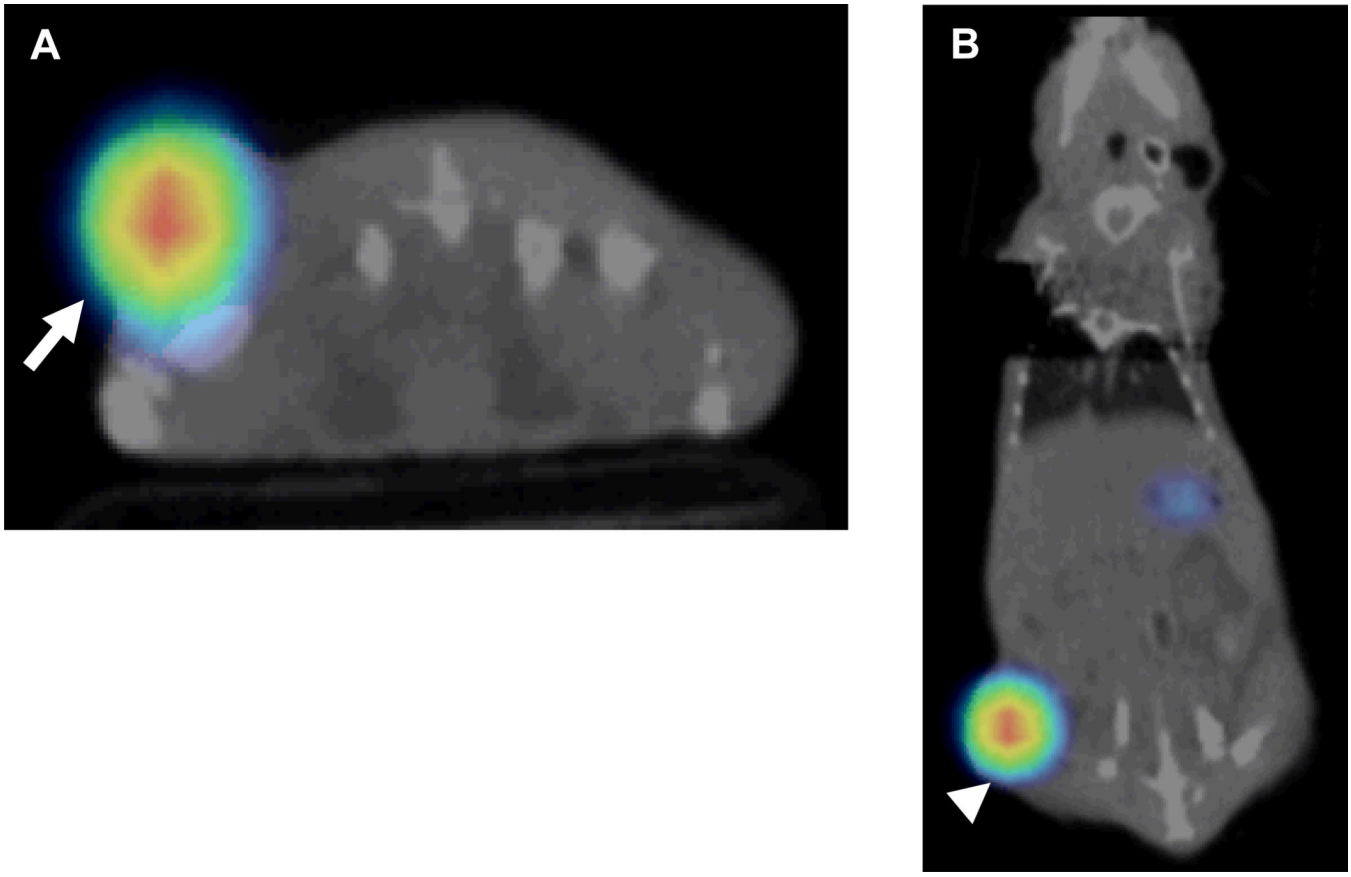

Fig. 6. Mouse with stable *NIS*-expressing right flank tumor

A and **B,** Representative axial (**A**) and coronal (**B**) fused ^{123}I micro-SPECT/CT images show mouse with a stable *NIS*-expressing right flank tumor (*arrow*, **A** and *arrowhead*, **B**) (percentage ID/g = 37.5).

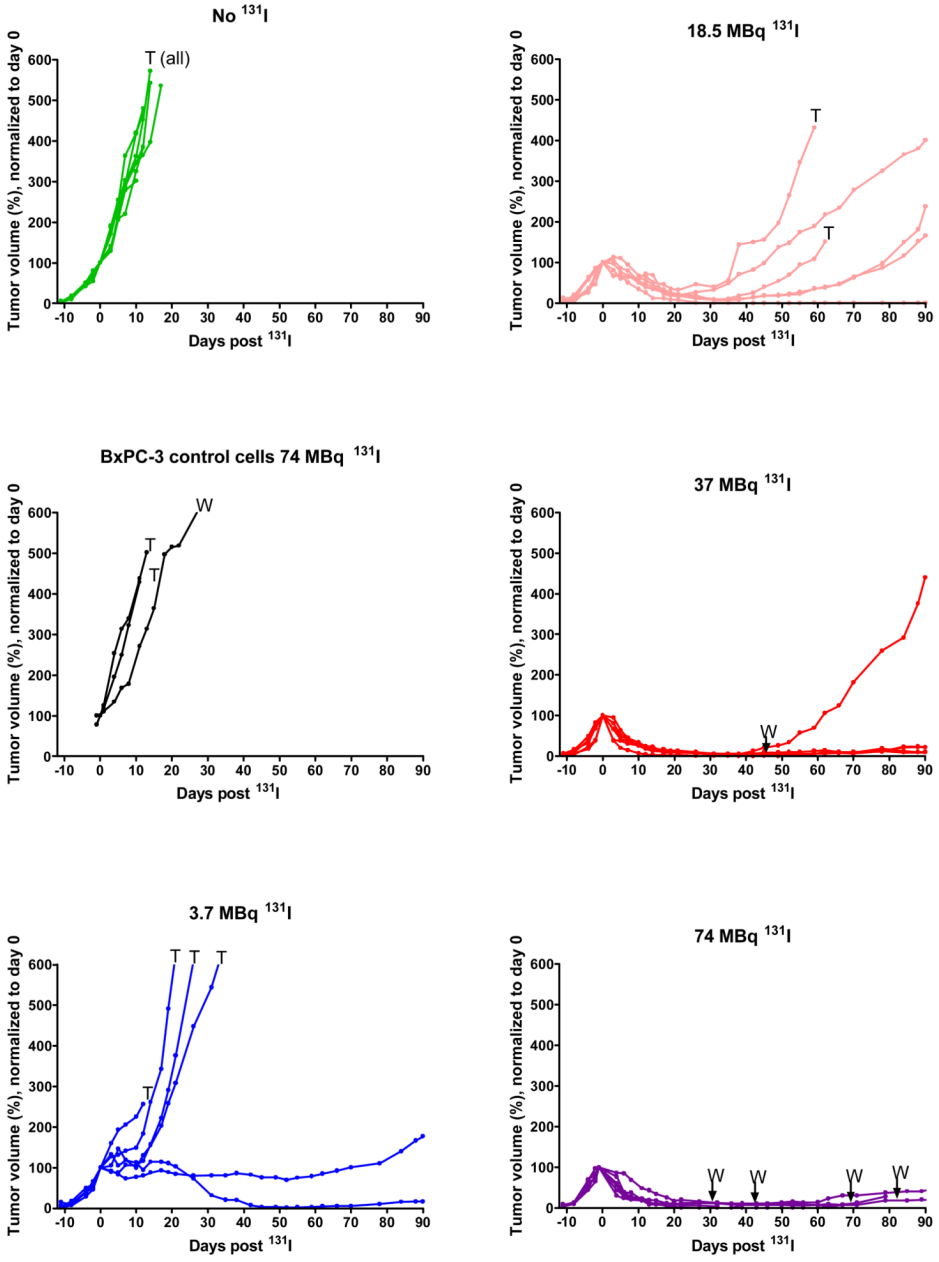

A

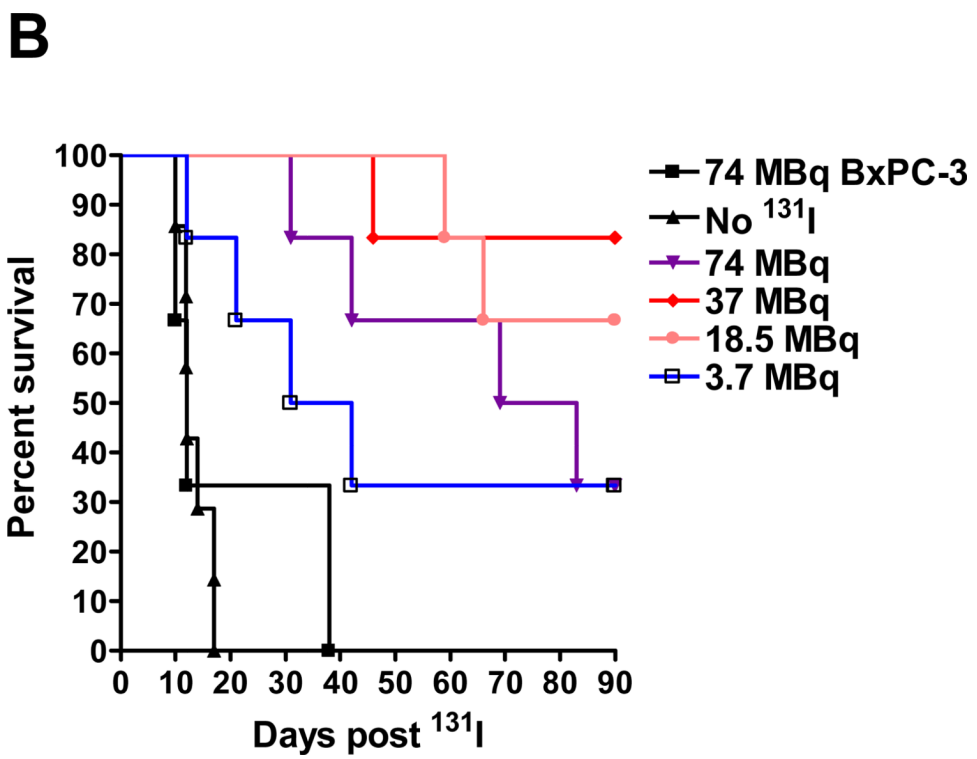

Fig. 7. ^{131}I radiotherapy study in stable *NIS*-expressing tumors

A–F, BxPC-3-*hNIS*-IRES-Em tumor volume measurements. **T** = mouse euthanized due to tumor volume ≥ 2 cm^3 or severe tumor ulceration due to rapid tumor growth, **W** = mouse died or euthanized due to extreme wasting, presumably secondary to ^{131}I toxicity. **G**, BxPC-3-*hNIS*-IRES-Em survival study. Graph shows significant prolongation of survival observed between BxPC-3-*hNIS*-IRES-Em tumor-bearing mice treated with 3.7 MBq versus no ^{131}I; however, difference was not significant versus the group of BxPC-3 control tumors given 74 MBq ^{131}I. Mice bearing BxPC-3-*NIS*-eGFP tumors which received 18.5, 37, and 74 MBq all exhibited significant prolongation of survival versus both control groups. There was no significant difference in survival between the 18.5, 37, and 74 MBq treatment groups.